Potential Energy Surfaces for the Reactions Si + O_2

Ivana Adamovic and Mark S. Gordon*

Department of Chemistry, Iowa State University, Ames, Iowa 50011

Received: May 18, 2004; In Final Form: July 2, 2004

This study investigates the reaction between silicon atom in its ground electronic state and ground-state molecular oxygen. The potential energy surfaces for the two competing reactions $Si(^3P) + O_2(^3\Sigma_g^-) = SiO_2(^1\Sigma_g^+)$ vs $Si(^3P) + O_2(^3\Sigma_g^-) = SiO(^1\Sigma_g^+) + O(^3P)$ are analyzed and compared. The lowest energy potential energy surface (PES) for each multiplicity is investigated within C_s symmetry. The entire potential energy surfaces were described using the multi-configuration self-consistent field (MCSCF) level of theory, augmented by multireference second order perturbation theory (MRMP2). Singles and doubles coupled cluster theory with perturbative triples, CCSD(T), energy calculations were also done at the MCSCF geometries. It is shown that the singlet reaction is thermodynamically favored, that the singlet product, SiO_2 ($^1\Sigma_g^+$), is the global minimum, and that both reactions have no net barrier. Extrapolation of the CCSD(T)/cc-pVTZ reaction enthalpies to the complete basis set (CBS) limit brings the calculations into excellent agreement with experimental data.

I. Introduction

Reactions between silicon and oxygen are of great importance in many areas of technology and chemistry. A very "vibrant" field in the past decade has been the development of nanotechnology[1a−e], in which silicon−oxygen clusters play an important role. Silicon-based optoelectronic devices[2a,2b] are just some of the possible applications for the silicon-oxides. Interest in the study of clusters vs bulk matter lies in the fact that nanostructures have different (and often more desirable) properties than the bulk system. Therefore, there has been considerable experimental[4a,4b] and theoretical[4a,4b,5,6] effort to understand and explain properties of silicon−oxygen compounds by studying small clusters. Of particular difficulty in cluster studies, from an experimental point of view, is the lack of direct methods to determine cluster electronic structure. Therefore, accurate examination of clusters is very important for theory. As mentioned above, several theoretical investigations have been performed on Si−O clusters; some of these studies[6a−d] have focused on a systematic description of cyclic Si−O compounds. There are also some studies of the reactions[7a−c] between different SiO compounds to form larger clusters.

The singlet analogue of reaction 2 (below) is described in great detail in a very recent publication.[8] Using the multireference configuration interaction (MRCI) method, the authors of this paper generated a global potential energy surface (PES) for the lowest singlet ($^1A'$) state and focused on dynamics simulations and calculations of the temperature dependence of the rate constants for the singlet analogue of reaction 2. Their work predicts that linear $SiO_2(^1\Sigma_g^+)$ is the global minimum, in agreement with the results presented here. The present work focuses instead on a detailed comparison of the lowest singlet and triplet potential energy surfaces for reactions 1 and 2.

From a theoretical point of view, it is of crucial importance to have a systematic and accurate method for treating and predicting properties of small silicon−oxygen clusters. Our interest in studying Si−O clusters, and growth reactions that lead to the formation of larger clusters, lies in the need for a better understanding of the formation mechanisms and electronic properties, so that desirable features may be enhanced. This study is the first step in the systematic study of small Si−O clusters. It explores the mechanisms and energetics for the formation of the two silicon oxides, SiO and SiO_2. The reactions of interest in the present work are as follows:

$$Si(^3P) + O_2(^3\Sigma_g^-) = SiO_2\ (^1\Sigma_g^+) \quad (1)$$

$$Si(^3P) + O_2\ (^3\Sigma_g^-) = SiO(^1\Sigma_g^+) + O(^3P) \quad (2)$$

The main issues to be considered are the nature of the wave function across the potential energy surface, the net thermodynamic energy and enthalpy differences, and barrier heights for reactions 1 and 2.

II. Computational Details

All calculations presented in this work were performed using the GAMESS[9] electronic structure code, with the exception of the triplet CCSD(T) energy calculations obtained with MOLPRO.[10a−d] Closed-shell CCSD(T) calculations were carried out with the coupled cluster code recently introduced into GAMESS.[11]

Since both reactions involve O_2, which is intrinsically multiconfigurational, the potential energy surfaces were initially studied using multiconfigurational self-consistent field (MCSCF) wave functions,[12] with a full valence active space within the fully optimized reaction space[13,14] (FORS) model, for both the singlet and triplet surfaces. The full valence MCSCF active space consists of 16 electrons in 12 orbitals, denoted MCSCF(16,12). Four orbitals correspond to the Si 3p and 3s atomic orbitals, while the remaining eight correspond to two sets of 2s and 2p O orbitals. The 6-31G(d)[15] basis set was used for the MCSCF(16,12) geometry optimizations. This basis set is useful for a qualitative description of the MCSCF potential energy surface (PES). All transition states and minima were

* Corresponding author. Tel: 515-294-0452. Fax: 515-294-0105; 5204. E-mail: mark@si.fi.ameslab.gov or gordon@ameslab.gov.

10.1021/jp040360z CCC: $27.50
Published on Web 09/01/2004

confirmed by the calculation and diagonalization of the MCSCF Hessian (matrix of energy second derivatives). The intrinsic reaction coordinate (IRC) method was employed to follow the minimum energy path from a transition state to reactants and products. This was accomplished using the Gonzalez−Schlegel second-order integration method,[16] with a step size of 0.05 ((amu)$^{1/2}$ − bohr).

To account for dynamic correlation, energy corrections at the MCSCF/6-31G(d) geometries were obtained using multireference second-order perturbation theory[17,18] (MRMP2) with the cc-pVTZ[19] basis set. In addition, single point calculations using the same basis set were performed at all MCSCF stationary points with singles and doubles coupled cluster theory including perturbative triples, CCSD(T). To study basis set effects on the predicted potential energy surfaces, CCSD(T) calculations were also performed with the cc-pVDZ[19] and cc-pVQZ[19] basis sets, thereby facilitating extrapolation to the complete basis set limit.

III. Results and Discussion

First, consider the electronic states of the system. In C_{2v} symmetry, the O_2 $^3\Sigma_g^-$ ground-state becomes $^3A_2$, $^3B_1$, or $^3B_2$ depending on the choice of axes, and the ^3P_g ground state of silicon reduces to $^3A_2 + {}^3B_1 + {}^3B_2$. Coupling these silicon and oxygen states will give $^{5,3,1}A_1 + {}^{5,3,1}A_2 + {}^{5,3,1}B_2$ states. For the singlet reaction 1, the lowest energy product is $^1A_1$ SiO_2, so the ground-state surface is of the greatest interest. The corresponding C_s states were also studied since the C_{2v} symmetry path on the closed shell surface is symmetry forbidden for the first step of the reaction. To provide a consistent description of the entire PES for reaction 1, one needs to use a full valence FORS active space. Only the full valence active space can correctly describe the degeneracy of the singlet surfaces at the asymptotic limit of separate reactants. To quantitatively compare reactions 1 and 2, the triplet surface was also treated using MCSCF(16,12) in C_s symmetry. Treatment of the triplet reaction in C_s symmetry allows the rearrangement of Si + O_2 to SiO and O.

A. Thermodynamics. First, consider the thermodynamics of the possible Si + O_2 reaction paths. Experimental enthalpies of formation[20] were used to estimate the experimental enthalpy of reactions 1 and 2 at 298.15 K.

The experimental enthalpy change for reaction 1 is very exothermic, $\Delta H_1^{298.15} = -181 \pm 2$ kcal/mol. Based on the Hammond postulate,[21] this reaction is therefore expected to have a small activation barrier. At the MCSCF(16,12) level of theory, using the cc-pVTZ basis set, the calculated change in enthalpy is $\Delta H_{1\mathrm{MCSCF}}^{298.15} = -154.9$ kcal/mol. This value has been corrected for zero point vibrational energy and scaled from 0 to 298.15 K, using translational, rotational (rigid rotator), and vibrational (harmonic) energy contributions calculated from the partition functions. The corresponding MRMP2 result, using the MCSCF geometries and temperature corrections, is $\Delta H_{1\mathrm{MRMP2}}^{298.15} = -161.8$ kcal/mol; this result is in close agreement with the CCSD(T) value, $\Delta H_{1\mathrm{CCSD(T)}}^{298.15} = -163.2$ kcal/mol. As expected, MCSCF underestimates the heat of reaction because of the lack of dynamic correlation. The agreement between multireference MRMP2 and single reference CCSD(T) illustrates the importance of dynamic correlation effects on the singlet surface, effects that are equally well represented by the two methods. Still, both methods differ by about 20 kcal/mol from the experimental value. It is shown in Section III B that basis set deficiencies are primarily responsible for this lack of agreement with experiment, and that use of an adequate basis set brings the CCSD(T) relative energies into excellent agreement with experimental values. However, these basis set effects have no impact on the key conclusions of this work.

TABLE 1: Structural Parameters for Reaction 1 (all optimizations done with MCSCF/6-31G(d))

	Si−O distance (Å)	O−Si−O angle (degrees)
P	1.529	180.0
TS	1.687	96.2
LM	1.689	58.1

TABLE 2: Dynamic Correlation and Basis Set Effects on $\Delta H_{298.15K}$ for Reaction 1

	cc-pVTZ			6-31G*	
	MCSCF	MRMP2	CCSD(T)	MCSCF	MRMP2
P	−154.9	−161.8	−163.2	142.9	−148.2
TS	−83.4	−78.4	−85.1	−77.7	−74.0
LM	−111.1	−96.2	−107.4	−104.2	−88.2
R	0.0	0.0	0.0	0.00	0.00

The experimental enthalpy for reaction 2 is $\Delta H_2^{298.15} = -72.0$ kcal/mol. The calculated MCSCF and MRMP2 values are $\Delta H^{298.15}{}_{\mathrm{MCSCF/6-31G^*}} = -88.9$ kcal/mol, $\Delta \mathrm{H}^{298.15}{}_{\mathrm{MCSCF/cc-pVTZ}} = -92.0$ kcal/mol, $\Delta H^{298.15}{}_{\mathrm{MRMP2/6-31G}} = -53.6$ kcal/mol, and $\Delta H^{298.15}{}_{\mathrm{MRMP2/cc-pVTZ}} = -53.8$ kcal/mol. In comparison, $\Delta H^{298.15}{}_{\mathrm{CCSD(T)/cc-pVTZ}} = -69.5$ kcal/mol and $\Delta H^{298.15}{}_{\mathrm{CCSD(T)/aug-cc-pVTZ}} = -70.5$.kcal/mol. So, the basis set effect on the triplet surface is much smaller than that for the singlet surface, and CCSD(T) is in much better agreement with the experiment than MRMP2. The extrapolation of the CCSD(T) reaction enthalpy to the basis set limit is discussed in Section III C.

Even though there are quantitative differences, all levels of theory predict that reaction 1 is more exothermic than reaction 2 by about 100 kcal/mol, in agreement with experiment. Thermodynamic considerations clearly favor formation of SiO_2 ($^1\Sigma_g^+$), in agreement with Dayou and Spielfiedel.[8] The next step in understanding reactions 1 and 2 is to examine the singlet and triplet potential energy surfaces (PES) in the relevant states. Once these PESs are determined, activation energies are considered to assess the relative kinetics for reactions 1 and 2. This is discussed in the next section.

B. Potential Energy Surfaces. Analysis of the low-lying singlet potential energy surfaces reveals that the lowest state is $^1A_1$. Therefore, for reaction 1, details are reported only for the $^1A_1$ state. The triplet surfaces were followed in C_s symmetry. Linear structures were also examined, but the C_s path is lower in energy, and during optimization, the linear structure transforms to C_s symmetry without a barrier. The electronic states of interest on the triplet surface are $^3A''$ and $^3A'$. At the limit of separate reactants and products, these two states are degenerate (same asymptote), but there is a small energy difference along the reaction path; therefore both states were considered along the entire reaction path.

$^1A_1$ Potential Energy Surface. Going from SiO_2 toward the separate reactants, two Si−O bonds break and the O−O bond forms. The formation of SiO_2 from Si+O_2 was followed in C_{2v} symmetry. The geometry parameters of these species are given in Table 1. Figure 1 shows a schematic of the stationary points along the PES. A transition state (TS) connects SiO_2 with a local minimum (LM). As may be seen in Table 1, the TS is structurally very similar to the LM but has a larger O−Si−O angle. There is no energy barrier separating the separated reactants from the local minimum.

The relative MCSCF, MRMP2, and CCSD(T) energies of SiO_2, TS, LM and separate reactants, using the cc-pVTZ and

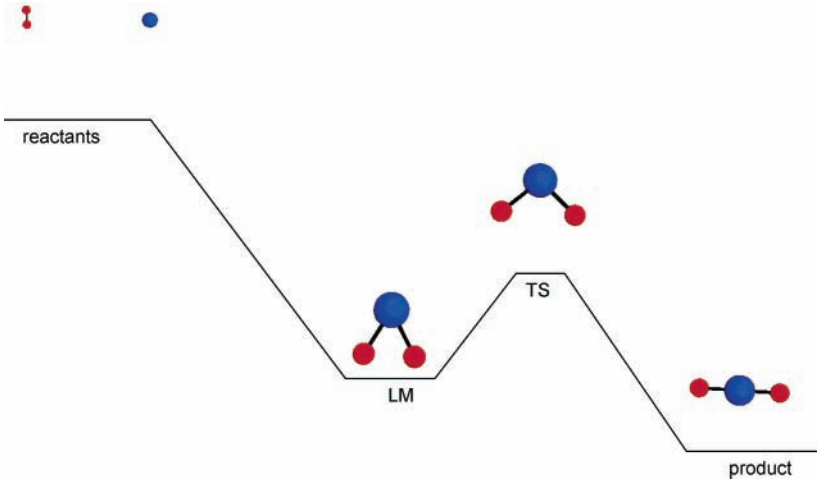

Figure 1. Schematic of the $^1A_1$ ($^1A'$) MCSCF potential energy surface.

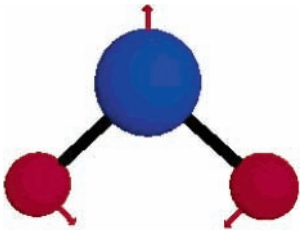

Figure 2. Transition-state geometry and imaginary frequency mode of the $^1A_1$ state.

6-31G* basis sets are given in Table 2. For the singlet surface basis set effects are very important, as can be seen from Table 2; more details on the basis set analysis are given in Section III C. The CCSD(T) and MRMP2 results exhibit similar trends, with differences in relative energies from 2 to 9 kcal/mol. The overall agreement between the two dynamic correlation methods for all relevant features on the singlet surface is very good. The activation energy connecting LM to product is ~28, 18, and 22 kcal/mol, as predicted by MCSCF, MRMP2, and CCSD(T), respectively. MCSCF overestimates the barrier, while the two dynamic correlation methods are in reasonable agreement. Note that the ~20 kcal/mol barrier is still well below the separated reactants. So, in agreement with the previous study,[8] there is more than enough energy available to reach the final product.

The next step in understanding the PES is to connect the LM with the separate reactants. Group theory considerations suggest that this part of the PES must have lower symmetry since the C_{2v} path is symmetry forbidden.[22] To establish that there is no barrier separating the reactants and LM, a series of MRMP2 single point energies were calculated along the C_s path. This path was determined by r, the distance from Si to the O−O midpoint, R, the O−O distance, and α, the angle between r and R. These calculations show that there is, indeed, no barrier for this part of the reaction. This is not surprising in view of the huge difference in energy (~100 kcal/mol) between the separated reactants and local minimum.

The normal mode corresponding to the imaginary frequency (759i cm^{-1}) for the singlet transition state is shown in Figure 2. An IRC calculation from this TS connects it with the final product, SiO_2, and with the LM.

$^3A''$ Electronic State. Now consider the $^3A''$ surface. Table 3 lists the MCSCF/6-31G(d) geometries of all stationary points along the reaction pathway, and Figure 3 illustrates a schematic of reaction 2. The relative energies for several levels of theory are given in Table 4. The influence of basis set is much smaller

TABLE 3: Structural Parameters of the Species Involved in Reaction 2 along the $^3A''$ Surface

	Si−O distance (Å)	Si−O−O angle (degrees)	O−O distance (Å)
P	1.534	70.7	3.975
TS	1.670	108.5	1.582
LM	1.736	108.8	1.422

TABLE 4: Dynamic Correlation and Basis Set Effects on $\Delta H_{298.15K}$ for Reaction 2 for the $^3A''$ Surface

	cc-pVTZ			6-31G*	
	MCSF	MRMP2	CCSD(T)	MCSCF	MRMP2
P	−92.0	−53.8	−69.5	−88.9	−53.6
TS	−37.6	−24.6	−31.9	−34.6	−23.9
LM	−38.3	−22.8	−34.7	−34.8	−22.3
R	0.0	0.0	0.0	0.0	0.0

than on the singlet surface, as described in detail in the next section. Dynamic correlation, taken into account with MRMP2 or CCSD(T), stabilizes the local minimum, TS, and reactants relative to the product by 20−30 kcal/mol. In contrast to the singlet PES, for which MRMP2 and CCSD(T) are in good agreement, these two methods differ by ~16 kcal/mol for the predicted reaction exothermicity. Adding zero point energy (ZPE) and temperature corrections (calculated with MCSCF/6-31G(d)) to MRMP2/cc-pVTZ reverses the order of TS and LM, so that TS is actually lower in energy by 1.8 kcal/mol. This suggests that the MRMP2 barrier is very small or zero so that LM may not exist on the $^3A''$ surface. CCSD(T) predicts a small, 2.8 kcal/mol, barrier separating the local minimum from products. This activation energy is much less than that in the case of the singlet surface (~20 kcal/mol). As for the singlet surface, the net exothermicity dominates the process, and there is no net barrier, as the TS is much lower in energy than the reactants.

For the part of the PES from the local minimum to separate reactants, an extensive transition state search did not locate a TS. Therefore, a series of constrained MCSCF optimizations was carried out starting from separate reactants and leading to the local minimum. Then, MRMP2 calculations were performed at each point on this linear synchronous transit (LST) path. This MRMP2/MCSCF LST path oscillates a little (no more than 1−2 kcal/mol) and then proceeds downhill to the local minimum with no barrier. It is therefore concluded that the path from reactants to local minimum has no intervening barrier, and that the small oscillations would disappear if the geometries along the LST path were reoptimized at the MRMP2 level of theory.

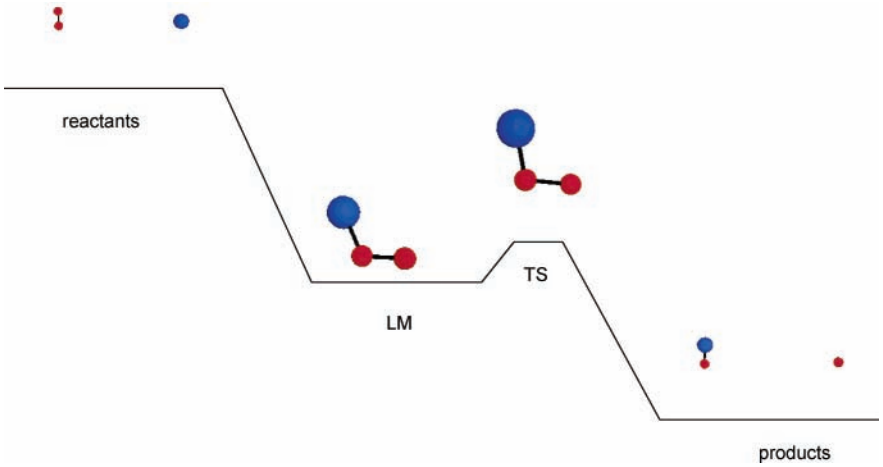

Figure 3. Schematic of the $^3A''$ MCSCF potential energy surface.

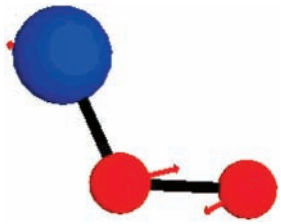

Figure 4. Transition-state geometry and imaginary frequency mode of the $^3A''$ state.

TABLE 5: Structural Parameters of the Species Involved in Reaction 2 along the $^3A'$ Surface

	Si−O distance (Å)	Si−O−O angle (degrees)	O−O distance (Å)
P	1.534	178.9	3.034
TS	1.666	116.9	1.556
LM	1.707	118.0	1.428

TABLE 6: Dynamic Correlation and Basis Set Effects on $\Delta H_{298.15K}$ for Reaction 2 for the $^3A'$ State

	cc-pVTZ			6-31G*	
	MCSF	MRMP2	CCSD(T)	MCSCF	MRMP2
P	−92.0	−53.3	−69.5	−88.9	−53.6
TS	−36.3	−23.8	−32.0	−36.2	−21.1
LM	−35.0	−20.9	−31.3	−37.7	−17.2
R	0.0	0.0	0.0	0.0	0.0

Figure 4 shows the TS, with its imaginary frequency of 983 cm^{-1}. The IRC method was employed to connect it with the appropriate minima.

$^3A'$ Electronic State. Geometries of all stationary points on the $^3A'$ surface are given in Table 5, and the relative energies are presented in Table 6. The local minimum and transition state in $^3A'$ symmetry are slightly higher in energy (∼2 kcal/mol) than those for the $^3A''$ species. The overall reaction path is similar to that represented in Figure 3.

The qualitative features of this PES are similar to that of the $^3A''$ state. In particular, there is a very small barrier separating the local minimum from products. This barrier is 1.5 kcal/mol for MCSCF, while for MRMP2 and CCSD(T), using MCSCF ZPE and temperature corrections, TS is lower in energy than LM by 1−3 kcal/mol. As noted before the only serious discrepancy between MRMP2 and CCSD(T) is in the overall reaction thermodynamics.

The search for a transition state between LM and reactants on the $^3A'$ surface followed the same procedure as that described for the $^3A''$ surface, with the same result: except for minor oscillations on the MRMP2/MCSCF surface, there appears to be no barrier between these two points.

TABLE 7: Relative CCSD(T) Energies for All Stationary Points on the $^1A^1$, $^3A''$, and $^3A'$ Surfaces (cc-p-V*n*Z (*n* = 2, 3, 4) (kcal/mol))

		cc-pVDZ	cc-pVTZ	cc-pVQZ	CBS	exp.
R		0.0	0.0	0.0	0.0	0.0
LM	$^1A_1$	−84.7	−107.4	−113.7	−122.3	
	$^3A''$	−24.5	−34.7	−37.9	−40.6	
	$^3A'$	−20.9	−31.3	−34.5	−37.2	
TS	$^1A_1$	−66.9	−85.1	−91.2	−95.9	
	$^3A''$	−22.9	−31.9	−33.9	−37.1	
	$^3A'$	−21.8	−32.0	−35.3	−37.8	
P	$^1A_1$	−134.2	−163.2	−171.3	−179.3	−181 ± 2
	$^3A''$	−59.6	−69.5	−72.7	−73.8	−72
	$^3A'$	−59.6	−69.5	−72.7	−73.8	−72

C. Basis Set Analysis. Since CCSD(T) usually predicts thermodynamic energy differences very accurately, it is likely that the discrepancy between the experimental and CCSD(T) reaction enthalpies on the singlet surface is a consequence of basis set deficiencies. Therefore, a systematic analysis of CCSD-(T) basis set effects was undertaken for both singlet and triplet potential energy surfaces. First, single point energies were calculated at the MCSCF(16,12) geometries, using the cc-pVDZ, cc-pVTZ, and cc-pVQZ basis sets.[19] Then, these CCSD(T) energies were extrapolated to the complete basis set (CBS) limit using an inverse cubic law expression.[23] The standard deviation for the fit is estimated to be in the range 0.1−1.0 mh.

Table 7 summarizes the relative CCSD(T) energies with the series of cc-pV*n*Z (*n* = 2, 3, and 4) basis sets, as well as the CBS and experimental values. All of the results were corrected for ZPE and temperature effects. $\Delta H_{CBS}^{298.3K}$ for the singlet surface is 179.3 kcal/mol, in excellent agreement with the experimental value of 181 ± 2 kcal/mol. For the triplet surface the reaction enthalpy is slightly improved relative to the cc-pVTZ result: 73.8 kcal/mol, for CCSD(T)/CBS vs the experimental value of 72 kcal/mol.

It is important to note that even though the basis set extrapolation dramatically improves the quantitative agreement with experiment, it does not alter any of the fundamental conclusions drawn in the previous sections.

D. Wave Function Analysis. Finally, consider the nature of the wave function as reactions 1 and 2 proceed. The first few doubly occupied orbitals, i.e., 2σ, 3σ, $2\sigma^*$, and $3\sigma^*$ orbitals on the oxygens and the 3s orbital (lone pair) on Si, do not change in the transition from the separate reactants to LM. The doubly occupied O_2 π_u orbital ultimately becomes a doubly occupied

O−Si−O π orbital. The doubly occupied π_u O_2 orbital combines with the empty Si $3p_z$ orbital to give a doubly occupied O−Si−O σ orbital. One of the singly occupied O_2 π_g* orbitals combines with a singly occupied Si p_x orbital to give a doubly occupied σ O−Si−O orbital. Finally, an electron from the remaining singly occupied Si p_y orbital (separate reactants) goes into the second, singly occupied O_2 π_g*, enhancing the antibonding between oxygens in LM. LM is a nearly closed shell system. The largest deviation of a natural orbital occupation number (NOON) from the closed shell value of 2.0 is 1.89, for the σ orbital on the oxygens. On the other hand, the TS is a singlet biradical (NOON from MCSCF calculations are 1.072 and 0.945, for the σ and σ* orbitals on the oxygens, respectively). The O−O bond is more broken here than in LM, so the oxygen σ and σ* orbitals are essentially singly occupied. In the final stage of the reaction these electrons combine with the lone pair (LP) from the 3s silicon orbital, so the final product is a closed shell (Hartree−Fock like) species.

The wave function analyses for the $^3A'$ and $^3A''$ states are very similar, so only the $^3A'$ is considered here. The transition from separate reactants into LM results in one singly occupied orbital each on Si and O atom. All species observed on the triplet surface are essentially single configurational, with the biggest variation of NOON from 0,1 or 2 being 1.896 and 0.114 for the σ bonding and σ* antibonding Si−O orbitals. The main feature of the triplet surface is the similarity between LM and TS, both in terms of geometry and electronic structure. The biggest change occurs during the rearrangement of the electronic structure in the transition from TS to product. An electron from the singly occupied p_x-p_y combination on silicon goes into an empty p_y orbital on one oxygen, so that it forms triplet oxygen atom and closed shell SiO.

IV. Conclusions

The two highest levels of theory employed in this study, MRMP2 and CCSD(T) predict the same general results. (1) SiO_2 ($^1\Sigma_g^+$) is the global minimum. (2) Both reactions 1 and 2 are very exothermic. (3) There is no net barrier on either singlet or triplet surfaces, so although reaction 1 is considerably more exothermic, both sets of products are kinetically accessible. (4) MRMP2 and CCSD(T) are in good quantitative agreement with each other and with experiment for the overall reaction energetics on the singlet surface, whereas this agreement deteriorates for the triplet surfaces. The latter is most likely due to the fact that dynamic correlation is much more important than nondynamic correlation for the triplet surface. Since the triplet surface has very little configurational mixing, it is likely that the CCSD(T) relative energies are more reliable than those from MRMP2. (5) The net enthalpy difference on the singlet surface is very basis set dependent; quantitative agreement with experiment requires extrapolation to the complete basis set limit.

Acknowledgment. This work was supported by a grant from the Air Force Office of Scientific Research. We are grateful to Dr. Michael W. Schmidt, Professor Kai-Ming Ho, and Professor Will A. Castleman, Jr. for useful discussions. For insights on the CBS analysis we thank Professor Klaus Ruedenberg and Dr. Laimutis Bytautas.

References and Notes

(1) (a) Bell, A. T. *Science* **2003**, 299, 1688. (b) Thornton, G. *Science* **2003**, *300*, 1378. (c) Canham, L. *Nature* **2000**, *408*, 411. (d) Appell, D. *Nature* **2002**, *419*, 553. (e) Gerstner, E. *Nature* **2003**, *425*, 244.

(2) (a) Dai, H. J.; Wong, E. W.; Lu, Y. Z.; Fan, S. S.; Lieber, C. M. *Nature* (London) **1995**, *375*, 769. (b) Han, W. Q.; Fan, S. S.; Li, Q. Q.; Hu, Y. D. *Science* **1997**, *277*, 1287.

(3) (a) Wang, L. S.; Nicholas, J. B.; Dupuis, M.; Wu, H.; Colson, S. D. *Phys. Rev. Lett.* **1997**, *78*, 4450. (b) Fan, J.; Nicholas, J. B.; Price, J. M.; Colson, S. D.; Wang, L. S. *J. Am. Chem. Soc.* **1995**, *117*, 5417.

(4) (a) Nayak, S. K.; Rao, B. K.; Khanna S. N.; Jena, P. *J. Chem. Phys.* **1998**, *109*, 1245. (b) Zhang, R. Q.; Chu, T. S.; Lee, S. T. *J. Chem. Phys.* **2001**, *114*, 5531 and references therein.

(5) (a) Bernstein, R. J.; Scheiner, S. *Int. J. Quantum Chem.* **1986**, *29*, 1191. (b) Nagase, S.; Kudo, T. *Organometallics* **1987**, *6*, 2456. (c) Schmidt, M. W.; Nguyen, K. A.; Gordon, M. S.; Montgomery, J. A., Jr. *J. Am. Chem. Soc.* **1991**, *113*, 5998. (d) Nguyen, K. A.; Carroll, M. T.; Gordon, M. S. *J. Am. Chem. Soc.* **1991**, *113*, 7924.

(6) (a) Snyder, L. C.; Raghavachari, K. *J. Chem. Phys.* **1984**, *80*, 5076. (b) Zachariah, M. R.; Tsang, W. *J. Phys. Chem.* **1995**, *99*, 5308. (c) Allendorf, M. D.; Melius, C. F.; Ho, P.; Zachariah, M. R. *J. Phys. Chem.* **1995**, *99*, 15285.

(7) Dayou, F.; Spielfiedel, A. *J. Chem. Phys.* **2003**, *119*, 4237.

(8) Schmidt, M. W.; Baldridge, K. K.; Boatz, J. A.; Elbert, S. T.; Gordon, M. S.; Jensen, J. H.; Koseki, S.; Matsunaga, N.; Nguyen, K. A.; Su, S. J.; Windus, T. L.; Dupuis M.; Montgomery, J. A., Jr. *J. Comput. Chem.* **1993**, *14*, 1347.

(9) (a) *MOLPRO*, a package of ab initio programs designed by H.-J. Werner and P. J. Knowles, version 2000; Amos, R. D.; Bernhardsson, A.; Berning, A.; Celani, P.; Cooper, D. L.; Deegan, M. J. O.; Dobbyn, A. J.; Eckert, F.; Hampel,C.; Hetzer, G.; Knowles, P. J.; Korona, T.; Lindh, R.; Lloyd, A. W.; McNicholas, S. J.; Manby, F. R.; Meyer, W.; Mura, M. E.; Nicklass, A.;Palmieri, P. ; Pitzer, R.; Rauhut, G.; Schütz, M.; Schumann, U.; Stoll, H.; Stone,A. J.; Tarroni, R.; Thorsteinsson, T.; Werner H.-J. (b) Hampel, C.; Peterson, K.; Werner, H.-J. *Phys. Lett.* **1992**, *190*, 1 and references therein. (c) Deegan, M. J. O.; Knowels, P. J. *Chem. Phys. Lett.* **1994**, *227*, 321. (d) Knowels, P. J.; Hampel, C.; Werner, H.-J. *J. Chem. Phys.* **1993**, *99*, 5219.

(10) Piecuch, P.; Kucharski, S. A.; Kowalski, K.; Musial, M. *Comput. Phys. Commun.* **2002**, *149*, 71.

(11) Schmidt, M. W.; Gordon, M. S. *Annu. Rev. Phys. Chem.* **1998**, *49*, 233.

(12) Roos, B. O.; Taylor, P. R.; Siegbahn, P. E. M. *Chem. Phys.* **1980**, *48*, 157.

(13) Ruedenberg K.; Schmidt, M. W.; Gilbert, M. M.; Elbert, S. T. *Chem. Phys.* **1982**, *71*, 41, 51, 65.

(14) (a) Hehre, W. J.; Ditchfield R.; Pople, J. A. *J. Chem. Phys.* **1972**, *56*, 2257. (b) Francl, M. M.; Pietro, W. J.; Hehre, W. J.; Binkley, J. S.; Gordon, M. S.; DeFrees, D. J.; Pople, J. A. *J. Chem. Phys.* **1982**, *77*, 3654.

(15) Gonzalez C.; Schlegel, B. H. *J. Phys. Chem.* **1990**, *94*, 5523.

(16) Nakano, H. *J. Chem. Phys.* **1993**, *99*, 7983.

(17) Hirao, K. *Chem. Phys. Lett.* **1992**, *190*, 374.

(18) (a) Dunning, T. H., Jr. *J. Chem. Phys.* **1989**, *90*, 1007. (b) Woon, D. E.; Dunning, T. H., Jr. *J. Chem. Phys.* **1993**, *98*, 1358.

(19) *CRC Handbook of Chemistry and Physics, 84th ed.*; Lide, D. R., Ed.; CRC Press: Boca Raton, FL, 2002.

(20) Hammond, G. S. *J. Am. Chem. Soc.* **1955**, *77*, 334.

(21) Woodward, R. B.; Hoffmann, R. *The Conservation of Orbital Symmetry*; Verlag Chemie: Weinheim/Bergstr./Academic Press: New York, 1971.

(22) Petersson G. A.; Frisch, M. J. *J. Phys. Chem. A* **2000**, *104*, 2183.